

VILNIUS UNIVERSITY
INSTITUTE OF CHEMISTRY OF CENTER FOR PHYSICAL SCIENCES AND
TECHNOLOGY

INGA STANKEVIČIENĖ

**SYNTHESIS AND COATINGS PRODUCTION OF
CARBONACEOUS NANOSTRUCTURES**

Summary of doctoral dissertation
Physical science, chemistry (03 P)

Vilnius, 2012

The work was carried out in Vilnius University in the period of 2006-2012

Scientific supervisor:

Prof. dr. Jurgis Barkauskas (Vilnius University, Physical sciences, Chemistry – 03P)

Scientific consultant:

Dr. Inga Grigoravičiūtė-Puronienė (Vilnius University, Physical sciences, Chemistry – 03P)

Evaluation board:

Chairman:

Prof. dr. Aldona Beganskienė (Vilnius University, Physical sciences, Chemistry – 03P)

Members:

Doc. dr. Ingrida Ancutienė (Kaunas University of Technology, Physical sciences, Chemistry – 03P)

Prof. habil. dr. Albertas Malinauskas (Center for Physical Sciences and Technology, Institute of Chemistry, Physical sciences, Chemistry – 03P)

Dr. Rasa Pauliukaitė (Center for Physical Sciences and Technology, Institute of Physics, Physical sciences, Chemistry – 03P)

Doc. dr. Artūras Žalga (Vilnius University, Physical sciences, Chemistry – 03P)

Official Opponents:

Doc. dr. Inga Čikotienė (Vilnius University, Physical sciences, Chemistry – 03P)

Doc. dr. Sigita Vėjelis (Vilnius Gediminas Technical University, Technological Sciences, Materials Engineering – 08T)

The official discussion will be held at 2 p.m. 5 October 2012 at the meeting of the Evaluation Board at the Auditorium of Inorganic Chemistry of the Faculty of Chemistry of Vilnius University.

Address: Naugarduko 24, LT-03225 Vilnius, Lithuania.

The summary of doctoral dissertation was mailed on the of September 2012.

The dissertation is available at the Library of Vilnius University and at the Library of Institute of Chemistry CPST.

VILNIAUS UNIVERSITETAS
FIZINIŲ IR TECHNOLOGIJOS MOKSLŲ CENTRO CHEMIJOS INSTITUTAS

INGA STANKEVIČIENĖ

ANGLINIŲ NANOSTRUKTŪRŲ SINTEZĖ IR DANGŲ GAMYBA

Daktaro disertacijos santrauka
Fiziniai mokslai, chemija (03 P)

Vilnius, 2012

Disertacija rengta 2006-2012 metais Vilniaus universitete

Mokslinis vadovas:

prof. dr. Jurgis Barkauskas (Vilniaus universitetas, fiziniai mokslai, chemija – 03P)

Konsultantė:

dr. Inga Grigoravičiūtė-Puronienė (Vilniaus universitetas, fiziniai mokslai, chemija – 03P)

Disertacija ginama Vilniaus universiteto Chemijos mokslo krypties taryboje:

Pirmininkas:

prof. dr. Aldona Beganskienė (Vilniaus universitetas, fiziniai mokslai, chemija – 03P)

Nariai:

doc. dr. Ingrida Ancutienė (Kauno technologijos universitetas, fiziniai mokslai, chemija – 03P)

prof. habil. dr. Albertas Malinauskas (Fizinių ir technologijos mokslų centro Chemijos institutas, fiziniai mokslai, chemija – 03P)

dr. Rasa Pauliukaitė (Fizinių ir technologijos mokslų centro Fizikos institutas, fiziniai mokslai, chemija – 03P)

doc. dr. Artūras Žalga (Vilniaus universitetas, fiziniai mokslai, chemija – 03P)

Oponentai:

doc. dr. Inga Čikotienė (Vilniaus universitetas, fiziniai mokslai, chemija – 03P)

doc. dr. Sigitas Vėjelis (Vilniaus Gedimino technikos universitetas, technologijos mokslai, medžiagų inžinerija – 08T)

Disertacija bus ginama viešame Chemijos mokslo krypties tarybos posėdyje 2012 m. spalio 05 d. 14 val. Vilniaus universiteto Chemijos fakulteto Neorganinės chemijos auditorijoje.

Adresas: Naugarduko 24, LT-03225 Vilnius, Lietuva.

Disertacijos santrauka išsiuntinėta 2012 m. rugsėjo d.

Disertaciją galima peržiūrėti Vilniaus universiteto ir FTMC Chemijos instituto bibliotekose.

1. INTRODUCTION

Since the first discovery of carbon nanotube (CNT) in 1991, CNTs have attracted much attention due to their outstanding physical and mechanical properties. CNT films and coatings are employed in nanoelectronics, biotechnology, sensing, filtration, etc. Graphene is a new material, which has attracted significant attention only recently. One encouraging aspect of graphene is to replace CNTs as a cheaper but better solution in various applications. Nowadays, CNTs and graphene are produced in large quantities by chemical vapor deposition (CVD) method. For practical purposes graphene is also produced from graphite oxide (GO).

Consequently, multi-walled carbon nanotubes (MWCNTs) were synthesized by the catalytic CVD method in the laboratory. As-grown CNTs inevitably contain carbonaceous impurities and remains of metal catalyst particles. To broaden the potential applications, highly efficient purification of the as-prepared CNTs is, therefore, very important. For this purpose a method prepared in the laboratory by using CCl_4 was applied to remove the residual Fe catalyst from the batch of synthesized CNT. Simultaneously, GO was synthesized from graphite powder by a Hummer's method.

At present time, there are many different methods for preparation of the coatings and films of nanometer-scale carbonaceous structures. In the laboratory the coatings of MWCNT were produced by the catalytic CVD method on the polished quartz and MgO substrates. Additionally, the coatings and films of nanometer-scale carbonaceous structures were fabricated from CNTs (as-grown and purified), GO and GO-CR (Congo red) aqueous suspensions. The coatings of MWCNT were fabricated on both MgO/PVA and epoxy resin (EP) substrates, whereas the coatings of GO and GO/CR were produced on polycarbonate (PC) membrane filter. These coatings can be easily transferred onto another substrate, or used as free-standing films for practical applications.

The aim of the research was to synthesize MWCNTs and GO and fabricate coatings thereof. For this reason there were the following tasks formulated:

1. To synthesize the MWCNTs using the catalytic CVD method and investigate the influence of synthesis parameters on the morphology of product. To purify the product using CCl_4 and $\text{H}_2\text{SO}_4/\text{HNO}_3$ mixture and assess the efficiency of purification methods.

2. To synthesize the GO by Hummer's method and characterize its structure.
3. To synthesize the MWCNT coatings directly grown by catalytic CVD method on the pellets of polished quartz and MgO substrate. To produce the CNT coatings on MgO/PVA and EP substrates from aqueous suspensions. To characterize the surface morphology of produced coatings.
4. To produce the GO and GO-CR aqueous suspensions and investigate the interaction between GO and CR molecules. To produce the GO and GO/CR films and coatings on the PC membrane filter, characterize the surface morphology and assess the CR influence on structure of coatings and films.

Statements for defence

1. The purification of CNTs by using CCl_4 is a suitable and an effective method to remove catalyst impurities. Moreover, this method can increase the chemical activity and the solubility in aqueous solutions without damaging the surface structure of CNTs.
2. The surface properties of the MWCNT coatings strongly depend on the nature of functional groups attached to the walls of CNTs. The surface of the coatings of as-grown MWCNTs is hydrophobic, while the surface modified with various functional groups indicates more hydrophilic character. The surface of the coatings produced from MWCNTs containing chlorine functional groups is non-polar with a big amount of acidic sites. The surface acidity increases after modification of CNTs with oxygen-containing functional groups.
3. The stability of GO aqueous suspensions is enhanced by interaction between GO particles and CR molecules. The properties of produced GO and GO/CR nanocomposite films and coatings depend on the GO to CR ratio and preparation conditions.

Scientific novelty

A method prepared in the laboratory using CCl_4 was successfully applied to remove the residual Fe catalyst from the batch of synthesized CNT.

For the first time residual Fe content in the purified CNT batches was determined by the magnetic balance method. Obtained data were applied to assess the remains of Fe

catalyst particles in both the synthesized and purified carbon samples. Moreover, we used the Eschka method for determination of the Cl position, bounded to CNT. This method of analysis was not used to investigate the carbonaceous structures.

A novel method for GO/CR nanocomposite films and coatings preparation by filtering through a PC membrane filter was developed in the laboratory.

The potentiometric titration method, which is based on Henderson-Hasselbalch equation was applied for the investigation of the GO and GO-CR mixtures.

2. EXPERIMENTAL

2.1. Methods of synthesis and purification of nanometer scale carbonaceous structures

2.1.1. Catalytic chemical vapor deposition of carbon nanotubes

The catalytic CVD method is the most common method of producing CNTs nowadays. It is widely used because of its low cost, high production yield and easy control of synthesis parameters. In order to control CNT diameter and purity, we varied the main several parameters: the catalyst precursor, reaction temperature, carbon source and additives. In the laboratory CNTs were synthesized using reaction parameters depicted below. Syntheses were classified by catalyst precursor.

CNTs synthesized using a carbonyl iron catalyst. CNTs were synthesized at 900 °C by a catalytic CVD method using carbonyl iron (size of particle 4,5–5,2 μm) and CH₄ as a catalyst and carbon source, respectively. The black colored product was collected from the ceramic boat.

CNTs synthesized using ferrocene. CNTs were synthesized using a 0,269 mol/l solution of ferrocene in *o*-xylene and CH₄. Ferrocene and *o*-xylene were used as a catalytic precursor and a carbon source, respectively. CH₄ acts both as a carbon feedstock and carrier gas. The synthesis procedure was carried out at the temperature of 900 °C. The resulting CNTs grew both on the pellets of polished quartz and on the inner surface of quartz reactor.

CNT coatings synthesized using pentacarbonyliron. The catalytic CVD method was performed using a 0,8–7,6 mol/l solution of pentacarbonyliron in toluene and CH₄. Pentacarbonyliron and toluene were used as a catalytic precursor and a carbon source

respectively, whereas CH₄ was used as both a carrier gas and carbon feedstock. The synthesis procedure was carried out at the temperature of 800–990 °C. The resulting CNTs grown on the pellets of polished quartz was collected from the center of reactor.

CNT coatings synthesized using Fe, Co and Ni phthalates and myristates. The coatings of CNT were synthesized on MgO substrates saturated with Fe, Co and Ni phthalates and myristates. In some cases an additive of (NH₄)₆Mo₇O₂₄ was used. The synthesis procedure was carried out at 800 °C. Carbon was deposited on the substrate of MgO and collected from the center of reactor.

CNTs synthesized using Fe, Co and Ni oxalates. CNT for the coatings formation was synthesized using Fe, Co and Ni oxalates prepared in the laboratory. The CNTs synthesis was carried out at 760–850 °C in CH₄ gas flow. Samples were collected from the ceramic boat. The metal catalyst from the synthesized samples was removed by dissolving in HNO₃.

2.1.2. Purification of carbon nanotubes

The samples of CNT were purified by treatment with CCl₄ gas and mixture of concentrated H₂SO₄/HNO₃ acids.

CCl₄ was used to remove the residual Fe catalyst from the batch of synthesized CNT and quartz pellets coated with carbon. The purification procedure was performed in the CVD reactor. Therefore, the samples placed in the center of reactor were heated for 60 min at 700 °C, under CCl₄/N₂ gas flow rate of 60 ml/min.

Additionally, CNTs were purified using a mixture of concentrated H₂SO₄/HNO₃ acids. This purification method was chosen in order to remove the catalyst impurities, modify the CNT walls with functional groups and increase the stability of their aqueous suspensions. The purification procedure was performed by stirring the CNTs in a mixture of acids for 30 min at 60 °C. After this time, the CNT/acid mixture was sonicated for 30 min. The functionalized CNTs were washed with distilled water using centrifugation several times until pH value reached 7. The deposits were dried in furnace at 50 °C to a constant weight.

The effectiveness of purification using CCl₄ gas treatment was investigated and compared this with H₂SO₄/HNO₃ treatment.

2.1.3. Synthesis of graphite oxide by Hummer's method

GO is the one of the most commonly used precursors to produce graphene. Therefore, in the laboratory GO was synthesized from graphite by a Hummer's method using NaNO_3 , H_2SO_4 and KMnO_4 . The oxidation product was washed with 10 % HCl solution and distilled water using filtration procedure. Precipitate was washed with distilled water using centrifugation. Washing process was repeated until the pH of the solution reaches ~ 6 . Obtained brown powder was dried in vacuum to a constant weight.

2.2. The methods of aqueous suspensions of nanometer scale carbonaceous structures production

2.2.1. Preparation of aqueous suspensions of carbon nanotubes

Aqueous suspensions of CNT were prepared by dispersing the particles in distilled water. Therefore, 0,25 g of as-grown and purified CNT were placed in 5,0 ml of distilled water and agitated for 24 h in a orbital shaker. Then, the CNT suspension was sonicated for 30 min. In order to suspend inherently hydrophobic CNTs (synthesized using a CoC_2O_4 and NiC_2O_4 as catalyst precursors) in an aqueous solution, 1 % sodium dodecyl sulfate (SDS) surfactant solution was added. Prepared 0,05 g/ml suspensions of CNT were used to fabricate coatings on EP and MgO/PVA substrates.

2.2.2. Preparation of aqueous suspensions of graphite oxide by Congo red dye addition

Aqueous suspensions of GO using a CR additive were prepared by dispersing the particles in distilled water. The required amount of GO was placed in 10,0 ml distilled water and agitated for 12 h in a orbital shaker. Then, the GO suspension was sonicated for 1 h, diluted to 100,0 ml and sonicated again for 1 h. An aliquot of 0,001 M CR solution was mixed with an appropriate volume of the stock solution of GO to prepare the GO-CR mixtures used for further investigations.

2.3. Production of carbonaceous coatings

2.3.1. Coatings made of carbon nanotubes

In the present work CNT coatings were prepared by two different methods. The first method was solution-based deposition of CNT coatings on MgO/PVA and EP substrates. The other method was the coatings preparation by catalytic CVD method directly growing on the polished quartz and MgO substrates.

2.3.2. Nanocomposite films and coatings made of graphite oxide and Congo red

The nanocomposite films and coatings of various GO to CR ratio were prepared from aqueous suspensions by filtering in water through a PC membrane filter (Table 1). Obtained GO/CR nanocomposite coatings and films were dried at room temperature, cut-off from the cylinder and used for further investigations.

Table 1 Percentage of CR in GO/CR nanocomposite samples

Sample	Mass % CR
GO1	0,00
GO2/CR	2,27
GO3/CR	4,44
GO4/CR	18,87
GO5/CR	31,75
GO5/CR*	31,75

2.4. Methods of investigation of carbon nanotubes, graphite oxide and produced coatings

The characterization of as-grown CNTs samples and GO/CR nanocomposite films were performed by scanning electron microscope (SEM) (EVO-50 EVP, Carl Zeiss). The samples of as-grown and purified CNTs were analyzed by using energy dispersive X-ray spectrometer (EDS) (Oxford instruments) equipment and magnetic balance designed in the laboratory on the basis of the analytical balance (KERN EG420-3NM) and 2 neodymium block magnets (K&J Magnetics). Residual Fe content in the purified CNT batches was determined gravimetrically. Raman spectra of CNTs samples were recorded using a Horiba Jobin Yvon LabRAM HR dispersive Raman microscope equipped with a He-Ne laser (633 nm), whereas Raman spectrum of GO and GO/CR

nanocomposites were obtained by FT-Raman spectrometer Spectrum GX (PerkinElmer Inc.) by using 1064 nm laser radiation. FT-IR spectra of the samples were recorded using a Perkin-Elmer FTIR Spectrum BXII instrument. UV–Vis absorption spectra were recorded using a Perkin Elmer Lambda 25 spectrometer in the range of 200–900 nm from aqueous solutions and dispersions of GO, GO-CR and CR. X-ray diffraction analysis (XRD) was performed using X-ray diffractometer D8 Advance (Bruker AXS) with Cu K α radiation, which was separated by a bent multilayer monochromator – Göbel mirror. Acidic functional groups on the surfaces of as-grown and purified CNTs have been determined by Boehm's titration. The Eschka method was used for the determination of the bounded to CNT Cl position. The potentiometric titration method, which is based on Henderson-Hasselbalch equation, was used for the investigation of GO and GO-CR mixtures. The way for describing neutralization in the systems containing liquid-solid interfaces is the application of the modified Henderson-Hasselbalch equation:

$$pH = pK_a + n \lg\left(\frac{\alpha}{1-\alpha}\right) \quad (1)$$

where pK_a stands for ionization constant, and α is a degree of ionization.

The linear fit of pH vs $\lg[\alpha/(1-\alpha)]$ gives pK_a and n (an index of accessibility of the ions to proton-exchange sites during the proton-exchange reactions). Additional information about the structure of colloidal particles can be obtained by plotting the variation of pK_a vs α , where pK_a stands for the intrinsic ionization constant, which is calculated at each pH value:

$$pH = pK_a + \lg\left(\frac{\alpha}{1-\alpha}\right) \quad (2)$$

The CNT coatings and GO and GO/CR nanocomposite films were examined using a contact angle measurement equipment (CAM200). In order to evaluate the surface energy, we used acid/base (van Oss) theory. The surface free energy components and subcomponents values of carbonaceous coatings and films were determined from the following equation system:

$$\left\{ \begin{array}{l} \gamma_{LA}(1 + \cos \theta_A) = 2 \left(\sqrt{\gamma_S^{LW} \gamma_{LA}^{LW}} + \sqrt{\gamma_S^+ \gamma_{LA}^-} + \sqrt{\gamma_S^- \gamma_{LA}^+} \right) \\ \gamma_{LB}(1 + \cos \theta_B) = 2 \left(\sqrt{\gamma_S^{LW} \gamma_{LB}^{LW}} + \sqrt{\gamma_S^+ \gamma_{LB}^-} + \sqrt{\gamma_S^- \gamma_{LB}^+} \right) \\ \gamma_{LC}(1 + \cos \theta_C) = 2 \left(\sqrt{\gamma_S^{LW} \gamma_{LC}^{LW}} + \sqrt{\gamma_S^+ \gamma_{LC}^-} + \sqrt{\gamma_S^- \gamma_{LC}^+} \right) \end{array} \right. \quad (3)$$

where S - solid, L - liquid, θ - contact angle, A, B and C - stands for appropriate liquids (water, glycerol and 1-bromnaphthalene), γ - surface total energy, γ^{LW} - non-polar Liftshitz-van der Waals interaction, γ^{AB} - polar Lewis acid-base interaction, γ^+ - electron-acceptor subcomponent, γ^- - electron-donor subcomponent.

According to the van Oss-Chaudhry-Good (vOCG) theory, γ_S of material can be expressed as the sum of two components, γ_S^{LW} and γ_S^{AB} :

$$\gamma_S = \gamma_S^{LW} + \gamma_S^{AB} \quad (4)$$

The latter (γ_S^{AB}) is expressed as the geometric mean of γ_S^+ and γ_S^- , and is given by:

$$\gamma_S^{AB} = 2\sqrt{\gamma_S^+ \gamma_S^-} \quad (5)$$

3. RESULTS AND DISCUSSION

3.1. Investigation of carbon nanotubes and graphite oxide

3.1.1. Analysis of carbon nanotubes

3.1.1.1. Analysis of as-grown carbon nanotubes

Reaction conditions are important factors that influence the morphology of product. Therefore the morphology of CNTs synthesized using the catalytic CVD method by changing main several parameters were examined by SEM. Furthermore, these samples were analyzed by EDS to assess elemental composition.

CNTs synthesized using carbonyl iron. Approximately 0,3 g of material was produced by the catalytic CVD method, using carbonyl iron as a catalyst precursor. The SEM images show that the resulting product composes of open-ended MWCNTs (Fig. 1a) and carbonaceous impurities (Fig. 1b). The analysis reveal that the tubes have diameter in the range 160–190 nm with the length exceeding 4 μm . EDS analysis indicated that this product consists of carbon (53,41 %), oxygen (4,59 %) and iron (42,00 %). Furthermore XRD measurements showed that the form of iron could either be

Fe_3C , $\text{Fe}_3(\text{CO})_{12}$ and cubic Fe (described in more details in chap. 3.1.1.2.). Supposedly, the oxygen detected is included in oxygen-containing functional groups on CNT surface.

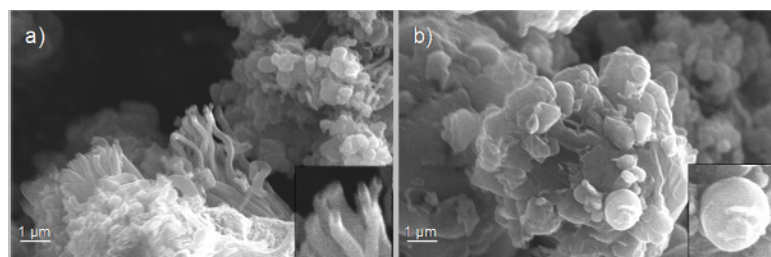


Fig. 1 SEM images of the MWCNT samples, synthesized on carbonyl iron: a) MWCNTs; b) carbonaceous impurities

CNTs synthesized using ferrocene. SEM images of CNTs formed on the walls of the quartz reactor are presented in Fig. 2. The SEM images reveal that the morphology of CNTs strongly depends on the sample's position (d is the distance from quartz tip of the syringe to the sampling location) in the reactor during synthesis procedure. The product formed at $d = 4,0\text{--}9,0$ cm ($T = 650\text{--}850$ °C) consists of 30–70 nm diameter entangled MWCNTs (Fig. 2a). At $d = 9,0\text{--}11,0$ cm ($T \approx 900$ °C) formed coral-like structures do not contain filamentous carbon (Fig. 2b). Downstream from the hottest peak zone at 650–850 °C formed carbon deposits are composed of entangled carbon nanotubes, which are uniform in diameter (70 nm; Fig. 2c).

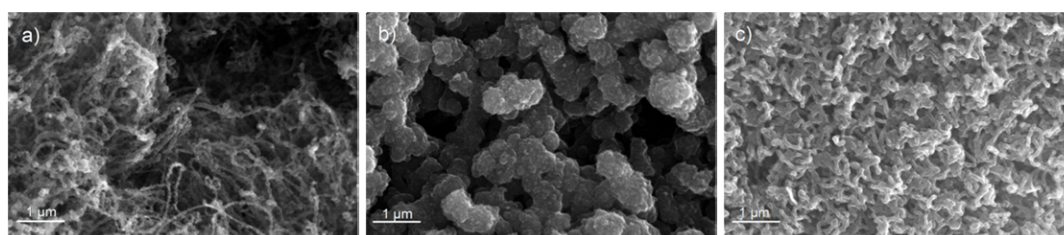


Fig. 2 SEM images of the samples deposited on the inner surface of the quartz tube: a) $d = 4,0\text{--}9,0$ cm; b) $d = 9,0\text{--}11,0$ cm; c) $d = 11,0\text{--}16,0$ cm.

EDS analysis showed position-dependent elemental constitution changes of the product (Fig. 3). The data revealed that synthesis product consists of carbon (87,64–91,26 %), oxygen (<7,29 %) and iron (1,45–7,86 %). XRD and Raman spectra of the as-grown samples showed that the impurities of iron present in the form of Fe_3C , Fe_4C , elemental Fe and Fe_2O_3 (described in more details in chap. 3.1.1.2.).

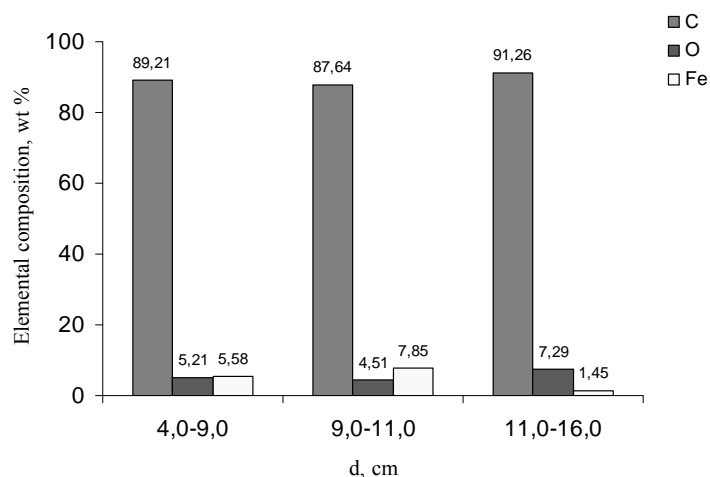


Fig. 3 EDS analysis of as-grown product

CNTs synthesized using Fe, Co and Ni oxalates. The morphology of as-grown product was different depending on the catalyst. The carbonaceous structures were not formed on the Fe catalyst at 800 and 850 °C. Fig. 4a shows the morphology of carbon filaments synthesized using a CoC_2O_4 catalyst precursor. The structure of the carbon filament there is quite different from that obtained in the previous experiments. The filaments (20 μm in diameter) are growing perpendicularly to the base surface; they are straight and brittle. Fig. 4b shows the SEM image of MWCNTs (<100 nm in diameter) synthesized at 780 °C using NiC_2O_4 catalyst precursor. Products were synthesized at 760 and 800 °C temperatures on Ni catalyst have the same morphology.

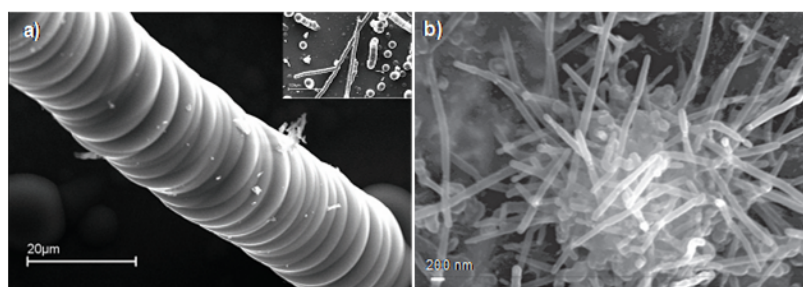


Fig. 4 SEM images of the product deposited using: a) CoC_2O_4 ; b) NiC_2O_4

The experimental results show that we obtained product with different morphologies by changing the reaction conditions. The >100 nm in diameter MWCNTs with a big amount of impurities were obtained in the synthesis using carbonyl iron (particle size 4,5–5,2 μm) as a catalyst precursor. The <100 nm in diameter MWCNTs were synthesized on the nanodispersed particles of Fe and Ni catalysts, which were

produced by thermal decomposition of ferrocene and NiC_2O_4 precursors, respectively. The optimal conditions to produce MWCNTs <100 nm diameter with the smallest amount of impurities are the catalytic reaction of ferrocene, *o*-xylene and CH_4 mixture at 650–850 °C.

3.1.1.2. Analysis of purified carbon nanotubes

In the laboratory the samples of CNT were purified by treatment with CCl_4 at higher temperatures, and mixture of concentrated $\text{H}_2\text{SO}_4/\text{HNO}_3$ acids. The purified samples were examined by using EDS, GA, XRD, FT-IR spectroscopy, Raman spectroscopy, Boehm's titration, Eschka titration methods and magnetic balance measurements. On this basis, the efficiency of the purification methods was assessed and compared.

CNTs synthesized using carbonyl iron. The elemental composition and Fe distribution in the samples of as-grown and purified CNTs is given in Table 2. Elemental analysis indicated that the content of chlorine after treatment with CCl_4 increased (up to 4,19 %). Also, the content of oxygen increased in the samples treated with the mixture of $\text{H}_2\text{SO}_4/\text{HNO}_3$ acids (7,33 and 10,42 %). Most probably functional groups were attached to the CNTs during purification procedures. The type and amount of the surface functional groups on CNTs were determined by the Boehm's titration method. The results of Boehm's titration show that the MWCNTs contain the greatest amounts of hydroxyl group (0,16 mmol/g), followed by carboxyl group (0,08 mmol/g), and then lactone group (0,02 mmol/g). Furthermore, the investigations of the functionalized samples show that the purified CNTs are more sensitive to oxidation than as-grown product. The amount and position of chlorine-containing functional groups bounded to CNTs surface were identified by the Eschka's method. The results of the analysis show that Cl- functional groups are directly bonded either to the cycle (2,90 %) or α -carbon of side chain (5,19 %).

The results of EDS, GA and magnetic balance measurements, indicating the presence of Fe, were compared in Table 2. Data in Table 2 show that as-grown CNTs contain ~40 % Fe and the amount of the impurities has decreased during purification procedure. The Fe catalyst is removed from the samples purified with CCl_4 more effectively.

Table 2 The data of EDS, GA and magnetic balance measurements of the samples of as-grown and purified CNTs (%)

Product	EDS					GA	Magnetic balance measurements
	C	O	Cl	S	Fe	Fe	Fe
S	53,41	4,59	0,00	0,00	42,00	38,00	39,00
V	91,87	2,46	4,19	0,00	1,48	1,20	0,85
NF	89,76	7,33	0,04	0,27	2,59	1,67	1,52
VF	88,00	10,42	0,49	0,53	0,55	0,00	0,65

Where S - as-grown, V – purified with CCl_4 , NF - as-grown functionalized (treated with $\text{H}_2\text{SO}_4/\text{HNO}_3$ acids), VF – purified functionalized samples

The FT-IR spectra of CNTs purified with mixture of $\text{H}_2\text{SO}_4/\text{HNO}_3$ acids is presented in Fig. 5a. The spectra indicate bands at wave number 3400 cm^{-1} (O–H stretching vibrations) of hydroxyl group. Bands in the $1652\text{--}1458\text{ cm}^{-1}$ range can be assigned to C=C bond of aromatic rings, whereas the band at 1706 cm^{-1} prove the presence of carboxyl functional group (stretching vibrations of C=O bond). Deformation vibrations of C–O bond observed at 1103 cm^{-1} and deformation vibrations of C=C bond in aromatic rings observed at 685 cm^{-1} . However the peak at 2362 cm^{-1} was attributed to CO_2 coating of IR optics in the spectrometer. FT-IR revealed the presence of hydroxyl and carboxyl functional groups on the CNT surface.

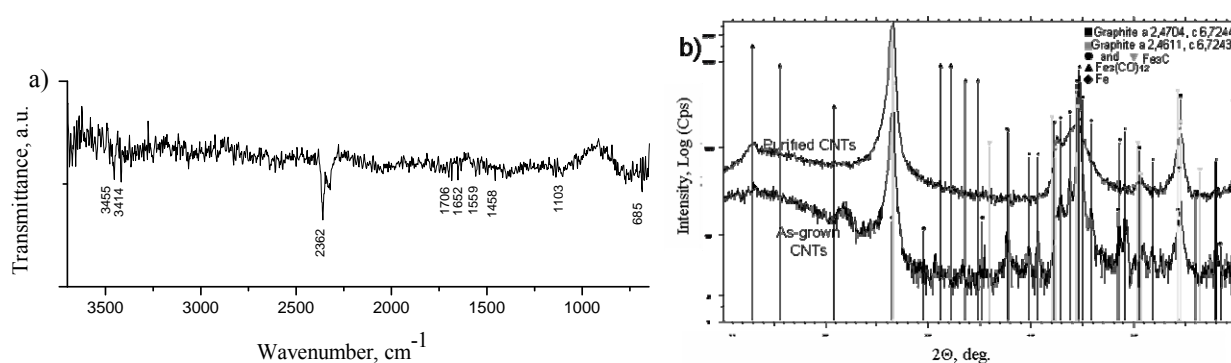


Fig. 5 a) FT-IR spectrum of functionalized MWCNTs; b) X-ray diffractograms of as-grown and purified with CCl_4 CNTs

The X-ray diffractograms of the as-grown and purified with CCl_4 samples are presented in Fig. 5b. In the XRD patterns the strong and broad peak at $2\theta \approx 26,5^\circ$ reveals graphite-like structure of the samples. The weak peaks at $2\theta \approx 42,0, 44,5, 50,5$ and $53,5^\circ$ corresponds to the diffraction of the (100) (100), (101), (102) and (004) planes, respectively. The result shows no significant difference between samples of as-grown

and purified (by CCl_4) CNT. In addition, the peaks corresponding to Fe_3C , $\text{Fe}_3(\text{CO})_{12}$ and cubic Fe were detected in the samples of as-grown CNTs. In the X-ray diffractogram of purified sample these peaks were not detected. This suggests that Fe impurities are effectively removed from CNT batch during the purification procedure.

CNTs synthesized using ferrocene. The elemental composition and Fe distribution in the samples of as-grown and purified CNTs, synthesized using ferrocene as a catalyst precursor and collected from the inner surface of the quartz reactor, is given in Table 3. The results of EDS analysis indicated an increased content of Cl (6,55 %) and O (20,34 %) after purification of samples with CCl_4 and $\text{H}_2\text{SO}_4/\text{HNO}_3$, respectively. Boehm titration method was used to determine the type and amount of oxygen-containing groups on the surface of oxidized CNTs. The results of Boehm titration show, that hydroxyl (0,29 mmol/g), carboxyl (0,14 mmol/g), and lactone (0,04 mmol/g) functional groups are attached to CNTs during purification procedure with the mixture of acids. FT-IR spectroscopy was used to investigate the CNT samples of purified with CCl_4 . Fig. 6 shows FTIR spectra of as-grown and purified CNT samples. A new band appears at 670 cm^{-1} in the spectrum of the purified sample, which is assigned to the stretching vibrations of C–Cl group. The results of Eschka method indicate, that Cl–functional groups are bonded to the cycle (4,69 %) and α -carbon of side chain (1,99 %).

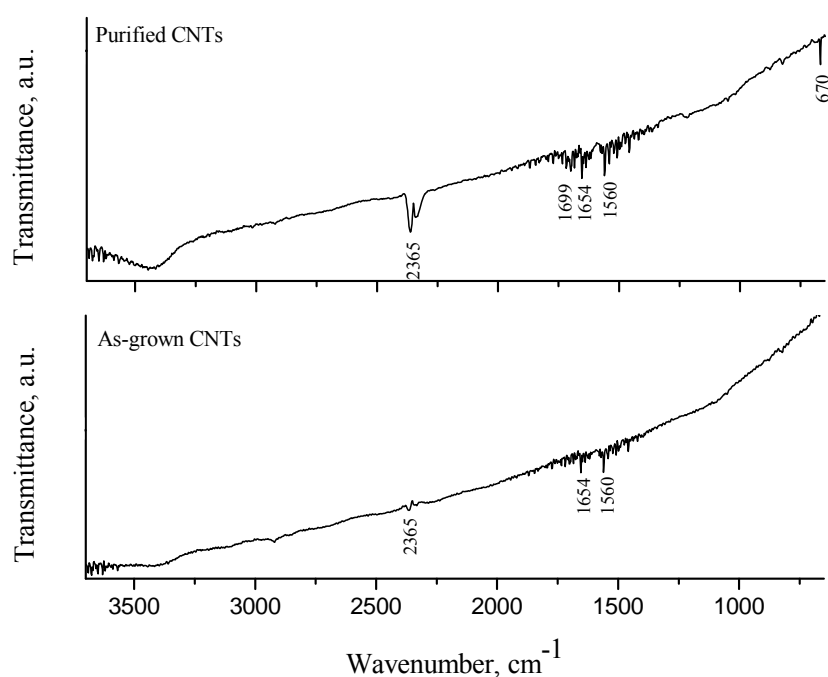


Fig. 6 FT-IR spectrum of purified with CCl_4 and as-grown CNTs

Table 3 The data of EDS, GA and magnetic balance measurements of the samples of as-grown and purified CNTs (%)

Product	EDS					GA	Magnetic balance measurements
	C	O	Cl	S	Fe	Fe	Fe
S	89,65	6,76	0,00	0,00	3,59	3,40	1,80
V	88,23	3,61	6,55	0,00	1,61	1,40	0,40
F	77,49	20,34	0,06	0,26	1,85	1,70	0,75

The results of EDS, GA and magnetic balance measurements show the presence of ~3 % of Fe impurities in the as-grown sample (Table 3). The amount of impurities decrease (up to ~1,4 %) during the functionalization procedure. Only traces of Fe are observed after treatment with CCl_4 .

Raman spectra of the as-grown and purified with CCl_4 samples are presented in Fig. 7. Peaks in the obtained Raman spectra show the presence of MWCNTs in the as-grown samples. D-band at 1300 cm^{-1} arises due to the disorder and defects in MWCNTs. G-band at $\sim 1600\text{ cm}^{-1}$ reflects lattice vibrations of the C–C bond. The G and D bands intensity ratio (I_G/I_D) indicate the high degree of crystallinity of as-grown and purified with CCl_4 product. Comparing the Raman spectra of the as-grown and purified CNT samples a conclusion about the minimal structural changes during the purification procedure can be made. A slight decrease of the D-band intensity observed after purification points to the reduction of defects in the walls of CNTs. This effect may be a consequence of the high-temperature treatment during the purification with CCl_4 . The low frequency bands at 500 cm^{-1} region can be attributed to Fe catalyst impurities in the Fe_2O_3 form of the as-grown sample.

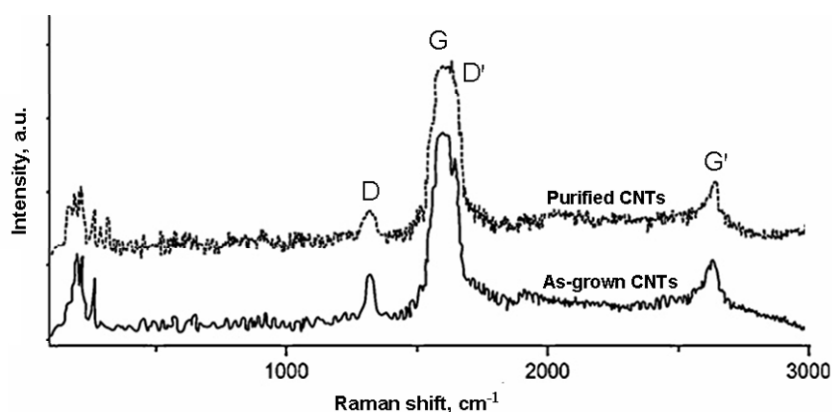


Fig. 7 Raman spectrum of purified with CCl_4 and as-grown CNTs

XRD patterns of the samples are presented in Fig. 8. The XRD patterns of as-grown and purified with CCl_4 samples show a characteristic peak of (002) phase of MWCNTs at $2\theta \approx 25,9^\circ$. The peak of (002) phase of functionalized CNTs are less shifted to $2\theta = 25,7^\circ$. This suggests that large amount of defects in nanotube walls were introduced during functionalization. Weak peaks at $2\theta \approx 42,5, 44,5, 50,5$ and $53,5^\circ$ can be assigned to the diffraction of the (100) (101), (102) and (004) planes, respectively. The d_{002} values derived from this XRD patterns are $\sim 3,4 \text{ \AA}$ for the as-grown and purified samples, while d_{002} value of functionalized sample is $\sim 3,5 \text{ \AA}$. Hence we may conclude that the interlayer spacing is expanded due functional group's attachment to CNTs during functionalization procedure. The size of crystallites are 67,0, 56,9 and 38,0 \AA of as-grown, purified and functionalized CNTs, respectively. That means the purification procedure almost does not affect structure of CNTs, whereas functionalization cuts CNTs into the smallest fragments. In addition, peaks corresponding to Fe_3C , Fe_4C and elemental Fe are detected in the samples of as-grown CNTs, while a weak peak corresponding to Fe_3C is detected in the sample of functionalized CNTs. In the X-ray diffractogram of purified CNTs these peaks are not detected. This suggests that Fe impurities are effectively removed from CNT batch during the purification procedure.

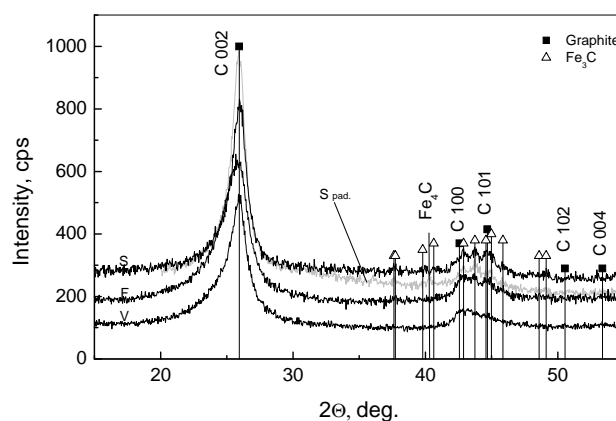


Fig. 8 X-ray diffractograms of as-grown (S), functionalized (F) and purified (V) CNTs and CNTs deposited on the pellet of polished quartz (S pad.)

The above results prove that the purification of CNTs by using CCl_4 is suitable and effective method to remove catalyst impurities. This method leads to surface modification with Cl- functional groups, which increases the chemical activity and the solubility in aqueous solvents without the damage of surface structure of CNTs. The

purification with $\text{H}_2\text{SO}_4/\text{HNO}_3$, in contrast to purification procedure with CCl_4 , cuts CNTs, damages the surface structure and introduces the oxygen functional groups on the walls of nanotubes.

3.1.2. Analysis of graphite oxide

The synthesized GO was analyzed by XRD, Raman spectroscopy, FT-IR spectroscopy, UV-Vis spectroscopy and pH-potentiometric titration methods.

The structure of GO was evaluated by XRD. In the XRD pattern of GO (Fig. 9a), the strong and broad peak at $2\theta = 11,04^\circ$ corresponds to an interlayer distance of $8,009 \text{ \AA}$ (d_{001}) for the AB-stacked GOs. Supposedly, the interlayer spacing of GO is expanded by H_2O molecules, intercalated between graphene sheets. The small peak at $2\theta \approx 42^\circ$ corresponds to the diffraction of the (100) plane. This means that the degree of crystallinity of GO is very low. These observations were confirmed by Raman spectroscopy (Fig. 9b). The significant structural changes occurring during the oxidation of graphite to GO are reflected in their Raman spectrum. The Raman spectra of the GO show G band at 1599 cm^{-1} and D band at 1338 cm^{-1} . These bands are blue-shifted and expanded in comparison with the bands of graphite. These results indicate reduction in the size of crystallinities due to the graphite oxidation. Moreover, these results show the significant decrease in the size of in-plane sp^2 domains. The intensity ratio of the G and D bands (I_G/I_D) reveals the high concentration of defects in GO structure.

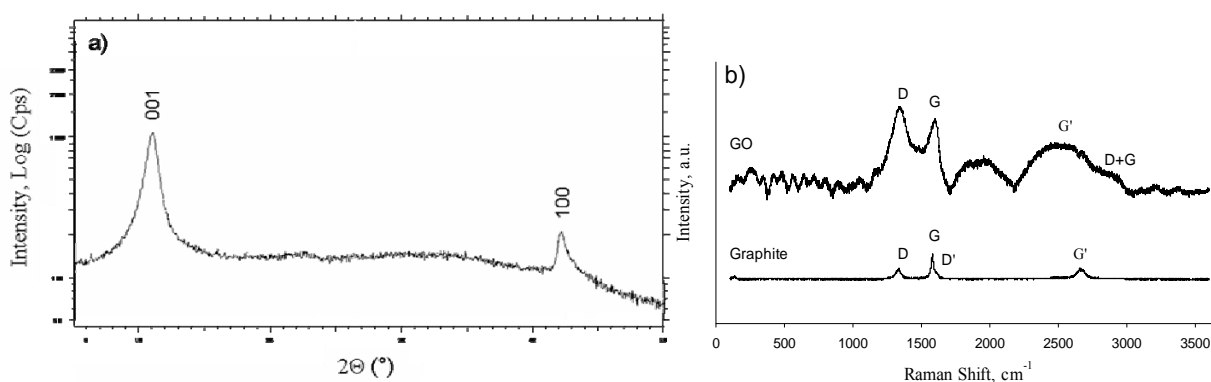


Fig. 9 a) XRD spectra of GO, b) Raman spectra of GO and graphite

Fig. 18a shows the FT-IR spectra of GO sample. FT-IR spectroscopy reveals the presence of hydroxyl, carboxyl, epoxy groups and non-oxidized regions in GO structure. These data were confirmed by UV-Vis spectroscopy analysis of GO suspension (the results of FT-IR spectroscopy and UV-Vis spectroscopy analysis in more details are

presented in chap. 3.2.2.2. and 3.2.2.1., respectively). Potentiometric titration experiments show that GO in aqueous solution behaves as a polyfunctional weak acid ($pK_a = 6,22$). There was also indicated a very big influence of electrostatic repulsion between functional groups (the results of potentiometric titration in more details are presented in chap. 3.2.2.1.).

3.2. Investigations of carbonaceous nano-structured films and coatings

3.2.1. Characterization of carbon nanotubes coatings

Characterization of CNT coatings produced on MgO/PVA, EP, polished quartz and MgO substrates were performed by CAM and SEM.

CNTs synthesized using carbonyl iron and ferrocene. The coatings fabricated from as-grown, purified and functionalized MWCNTs on MgO/PVA and EP substrates were analyzed by CAM. The results of CAM show that the coatings of as-grown MWCNTs are hydrophobic, while the coatings of functionalized MWCNTs are hydrophilic. The coatings formed from CNTs treated with CCl_4 exhibit a less hydrophilic character in comparing with the coatings formed from functionalized CNTs. The values of surface free energy components ($\gamma_S^{LW} > \gamma_S^{AB}$) show, that surface of CNTs coatings purified with CCl_4 are non-polar with a big amount of acidic sites ($\gamma_S^+ > \gamma_S^-$). The surface acidity increases after modification with oxygen containing functional groups. Also, it was found that EP substrate has an influence on the properties of the coatings formed on it.

CNT coatings synthesized using ferrocene. MWCNT coatings were prepared by catalytic CVD method directly growing on the polished quartz substrates located at different positions in the reactor. The SEM images show that the morphology of these coatings depends on the position of the sample in the reactor during synthesis procedure (Fig. 10). It is important to note that the formation of CNTs (40–100 nm in diameter) occurs only on 2, 3 and 5 substrates, located in the reactor $d = 4,0, 6,0$ and $12,5$ cm at $650\text{--}850$ °C. Furthermore, higher synthesis temperature induces the growth of larger diameter MWCNTs. Coral-like structures grow in the centre of the reactor (at $d = 9,0$ cm and $T \approx 900$ °C).

MWCNT coatings on the polished quartz substrates were successfully purified with CCl_4 . The as-grown and purified coatings were analyzed using CAM. The obtained data demonstrate the hydrophobic nature of as-grown MWCNT coatings, while the coatings treated with CCl_4 are more hydrophilic. The data presented in Fig. 11 indicate that the total surface energy of the coatings increase after purification procedure. It is important to note that the total surface energy values of the coatings of smaller diameter CNTs are higher than that of the larger diameter CNTs. Also, the data presented in Fig. 11 show that the surface of as-grown MWCNT coatings is non-polar ($\gamma_S^{LW} > \gamma_S^{AB}$) with a small amount of acidic and basic sites, whereas surface of the purified coatings is polar ($\gamma_S^{LW} < \gamma_S^{AB}$) with a big amount of acidic sites ($\gamma_S^+ > \gamma_S^-$).

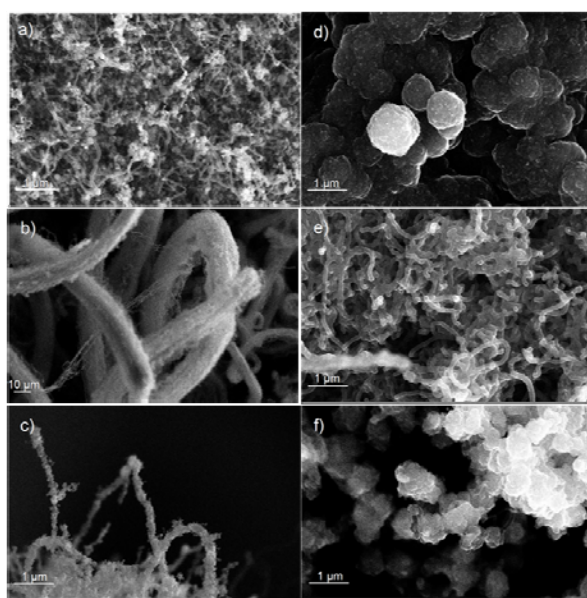


Fig. 10 SEM images of the CNT coatings on the polished quartz substrates: a) marked as pellet 2 ($d = 4,0$ cm); b) and c) marked as pellet 3 ($d = 6,0$ cm); d) marked as pellet 4 ($d = 9,0$ cm); e) marked as pellet 5 ($d = 12,5$ cm); f) marked as pellet 6 ($d = 14,5$ cm)

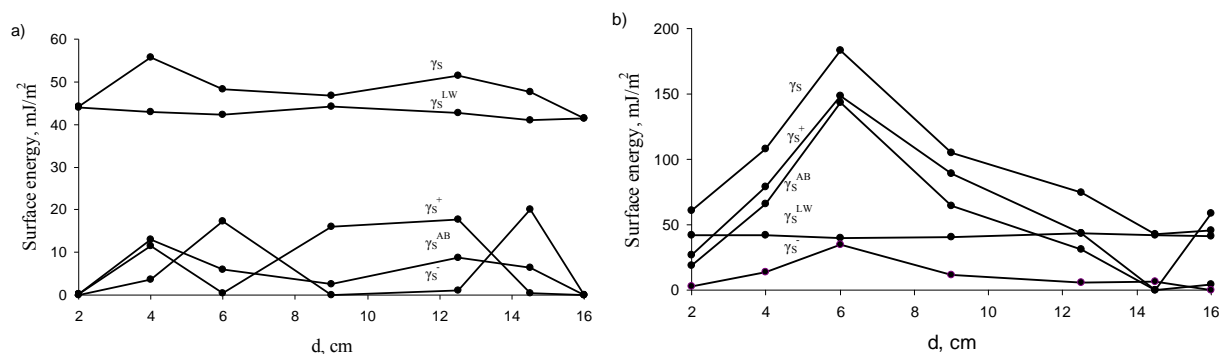


Fig. 11 Surface energy (in mJ/m^2) dependence on the samples position in the reactor (d) during synthesis procedure: a) as-grown CNTs; b) purified with CCl_4 CNTs

CNT coatings synthesized using pentacarbonyliron. CNT coatings were produced by catalytic CVD method directly growing on the polished quartz substrates located in the centre of the reactor. SEM images (Fig. 12) of the coatings reveal the morphology dependent on the synthesis temperature and concentration of catalyst precursor (toluene additive). SEM analysis shows that the synthesis temperature affects the average diameter of MWCNTs. In general, the CNTs' diameter increases with increasing growth temperature from 800 to 970 °C, and the CNTs' diameter reduces with increasing growth temperature from 970 to 990 °C. Moreover, it was found that the amount of carbonaceous impurities decreases with the increase of the temperature. Also, data from SEM analysis show that higher concentration of toluene induces the formation of larger diameter CNTs.

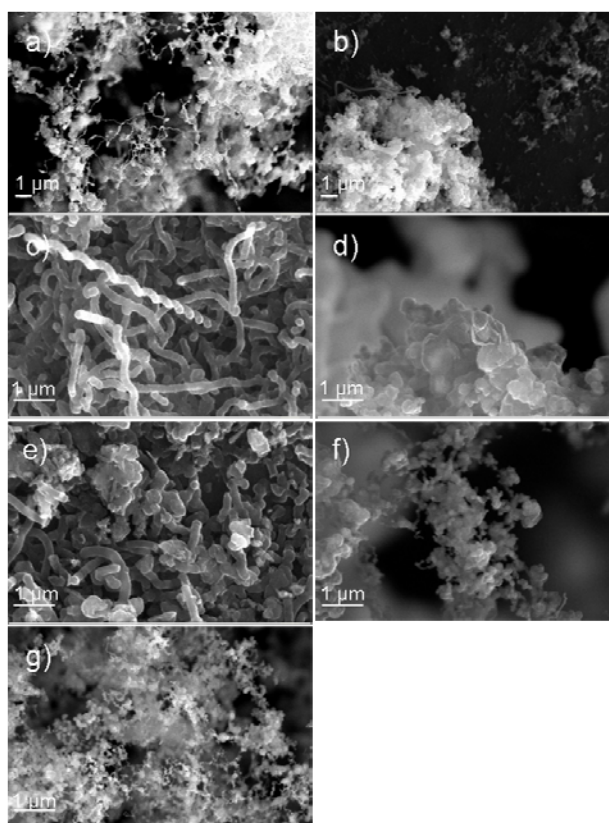


Fig. 12 SEM images of the as-grown CNT coatings on the polished quartz substrates. Synthesis temperature: a) and b) T = 900 °C; c) and d) T = 920 °C; e) and f) T = 970 °C; g) T = 990 °C. Concentration of catalyst precursor: a), d) and f) 7,6 mol/l; b) 3,8 mol/l; c) 0,8 mol/l; e) and g) 1,1 mol/l

CNT coatings synthesized using Fe, Co and Ni phthalates and myristates. CNT coatings were prepared directly growing by catalytic CVD method on the MgO

substrates. SEM images of these coatings are presented in Fig. 13. The morphology of nanostructured carbon coatings obtained on the Fe, Co and Ni catalysts strongly depends on the nature of precursor. In the presence of phthalates a web of CNTs in the matrix of amorphous carbon is obtained. The diameter of CNTs is in the range 5–30 nm (Fig. 13a, e and i). In the experiments with the myristates only the formations of amorphous carbon are clearly seen (Fig. 13c, g and k). In general, a conclusion that $(\text{NH}_4)_6\text{Mo}_7\text{O}_{24}$ additive acts adversely the formation of the filamentary carbon nanostructure can be done (Fig. 13b, f, j, d, h and l).

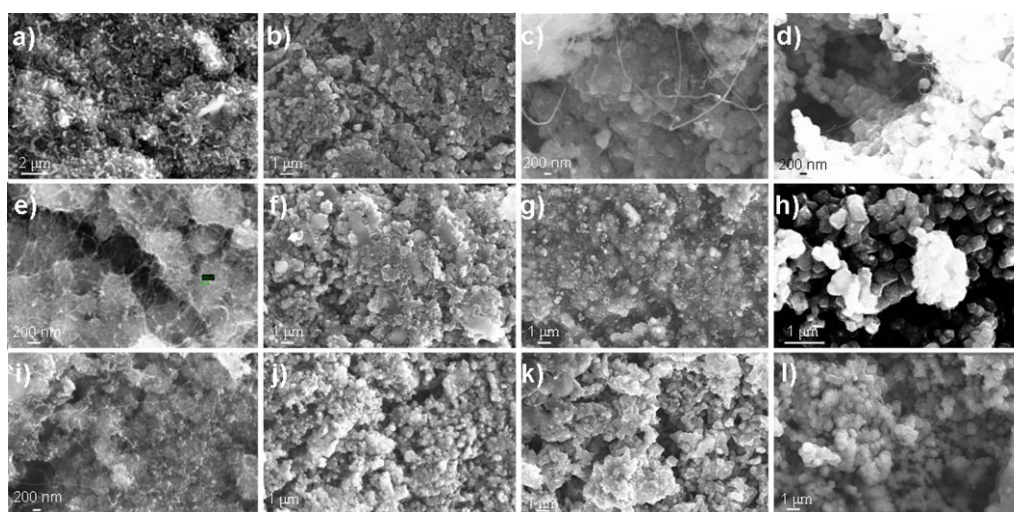


Fig. 13 SEM images of nanostructured carbon coatings on MgO substrate. Catalyst precursors: a) and b) $\text{FeC}_6\text{H}_4(\text{COO})_2$, c) and d) $\text{Fe}(\text{CH}_3(\text{CH}_2)_{12}\text{CO}_2)_2$, e) and f) $\text{CoC}_6\text{H}_4(\text{COO})_2$, g) and h) $\text{Co}(\text{CH}_3(\text{CH}_2)_{12}\text{CO}_2)_2$, i) and j) $\text{NiC}_6\text{H}_4(\text{COO})_2$, k) and l) $\text{Ni}(\text{CH}_3(\text{CH}_2)_{12}\text{CO}_2)_2$; b), f), j), d), h) and l) samples with $(\text{NH}_4)_6\text{Mo}_7\text{O}_{24}$ additive.

CNTs synthesized using Co and Ni oxalates. CNT coatings were fabricated on MgO/PVA substrate from aqueous suspensions and then were transferred on EP substrate for the investigations. The coatings were analyzed using CAM. Obtained data show that the coatings produced from material grew on Co catalyst, demonstrate the hydrophilic nature. On the contrary, coatings produced from CNTs grew on Ni catalyst have rather hydrophobic surfaces. The surface of coating prepared from material synthesized on Co is polar ($\gamma_S^{LW} < \gamma_S^{AB}$) with a prevailing electron-donating sites ($\gamma_S^+ < \gamma_S^-$), whereas the coatings formed from MWCNTs synthesized on Ni distinguished non-polar character with large amount of basics sites.

In summary the morphology of the CNT coatings strongly depends on the synthesis parameters (catalyst precursor and temperature). The surface properties of the coatings depend on the amount and nature of functional groups attached to CNTs' walls.

3.2.2. The investigation of interaction between graphite oxide and Congo red and characterization of the nanocomposite films and coatings

3.2.2.1. The characterization of interaction between graphite oxide and Congo red in aqueous media

Evidence for direct interaction between GO and CR is the change of the color of aqueous dispersions during sonication procedure. Therefore, interaction between GO and CR molecules in aqueous media was studied using potentiometric titration and UV–Vis spectroscopy methods.

The potentiometric titration method, which is based on Henderson-Hasselbalch equation was applied for the investigation of the GO and GO-CR aqueous dispersions. The obtained data are presented in Table 4.

Table 4 n and pK_a values, determined for GO and GO-CR mixtures using Henderson-Hasselbalch equation

Sample	n	pK_a
GO1	3,44	6,22
GO2-CR	3,84	6,49
GO3-CR	3,83	6,65
GO4-CR	2,78	6,61
GO5-CR	2,04	6,77
GO5-CR*	1,74	6,51

Values of n are much higher than 1 both for GO and for CO-CR mixtures in aqueous solutions, indicating a very big influence of electrostatic repulsion between functional groups. Value of n for GO equals 3,44 and reflects a rather complex structure of this compound with functional groups located in less accessible sites. Addition of a small amount of CR diminishes the accessibility of these active sites. Larger quantities of CR (18,87 % and more) are able to reduce the values of n . The values of pK_a gradually increase with addition of CR, being evidence that the ionization becomes more difficult. Information about the structure of colloidal particles can be obtained by

plotting the variation of pK_α vs α (Fig. 14). Deviations from the linear relationship have been traditionally interpreted as being indicative of conformational transitions upon ionization. The plot of pK_α vs α for pure GO is almost linear, which could be explained by small conformational transitions of GO sheets during the process of ionization. Small amounts of CR do not affect this process substantially, while higher CR ratio induce the more pronounced structural changes of colloidal particles during the ionization process.

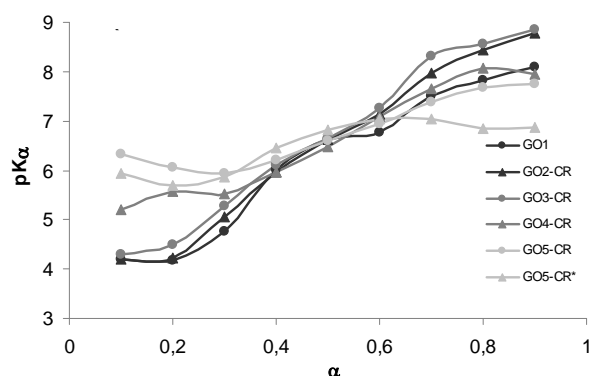


Fig. 14 Plots of pK_α vs α for GO and GO-CR mixtures in aqueous solutions

UV-Vis spectra of the GO and GO-CR samples are shown in Fig. 15. In the UV-Vis spectrum of GO two characteristic peaks at 240 nm (attributed to $\pi \rightarrow \pi^*$ transitions of aromatic C=C bonds) and 305 nm (ascribed to $n \rightarrow \pi^*$ transitions of C=O bonds) are observed (Fig. 15a). UV-Vis spectra of the CR basic solution show peaks at 423, 453 and 485 nm. They are assigned to the short-wavelength $\pi \rightarrow \pi^*$ transitions of the aromatic rings (benzene and naphthalene, respectively) and the $n \rightarrow \pi^*$ transitions of free electron pairs of the N atoms of the azo-group, respectively (Fig. 15a), and represent the structure shown in Fig. 16 (structure I). Appearance of the peak at 610 nm of CR solution in acidic media (Fig. 15a) is assigned to the transformation of the molecule (Fig. 16, structure II). Spectra of freshly prepared GO-CR* mixtures are quite similar to the spectra of pure CR in basic media (Fig. 15a). Available information suggests that there is no direct interaction between GO and CR in freshly prepared mixtures. The UV-Vis spectra of sonicated GO-CR mixtures are basically changed (Fig. 15b). The peaks at 240 and 305 nm appear more clearly in comparison with the spectra of the freshly prepared samples. Moreover, the new absorption bands at above 650 nm appear for the sample GO5-CR with the maximum content of the dye. This may be the evidence that direct interaction between GO particles and CR occurs during sonication procedure. The new

absorption bands of CR above 650 nm emerge due to the ammonium-azonium tautomerism (Fig. 16, structures III–VI). The peak at 493 nm disappears at the lower ratio of CR and appears only for the sample GO5-CR with the maximum content of the dye. Perhaps it is an indication of more intense interaction between GO and CR leading to the formation of GO-CR nanocomposites with higher ratio of CR.

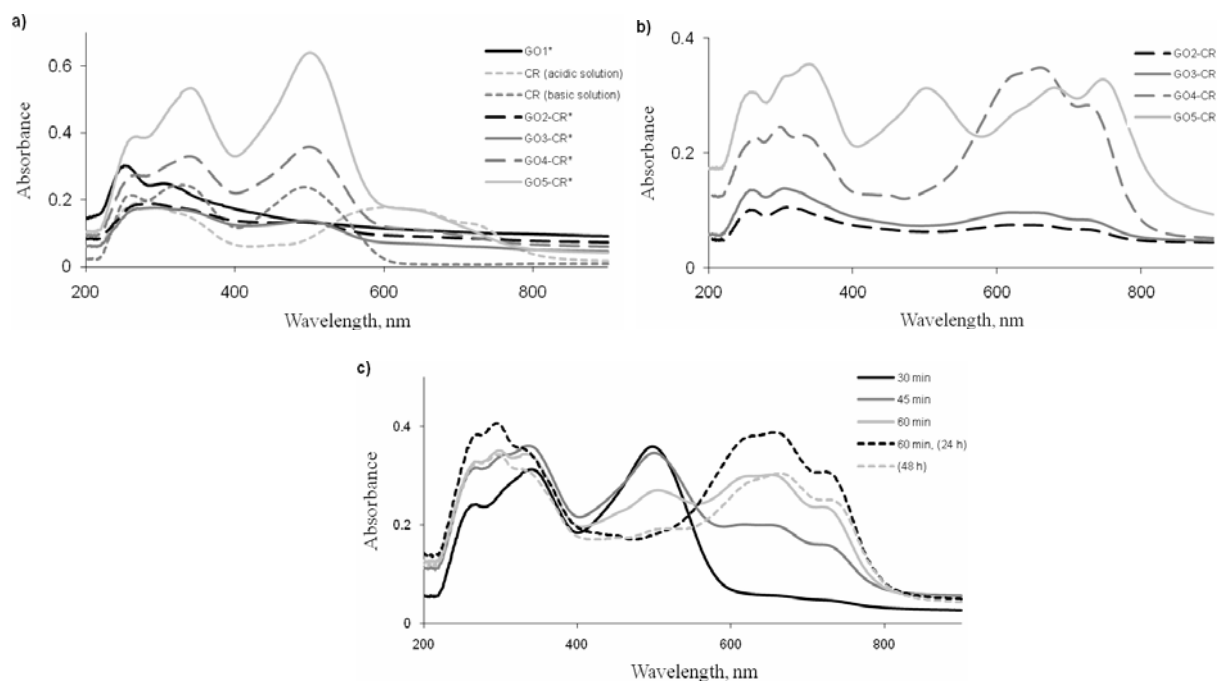


Fig. 15 UV-Vis spectra of GO and CR mixtures in aqueous solutions: a) spectra of pure GO, CR and non-sonicated GO-CR mixtures; b) spectra of sonicated (1 h) GO-CR mixtures; c) spectra of GO4-CR mixture after various time of sonication (given in minutes) and keeping (given in hours)

Influence of sonication time and keeping time on the spectral characteristics of GO4-CR mixtures has been studied (Fig. 15c). The altered intensity and shifting of bands indicates direct interaction between GO and CR appears after 48 h or 1 h of sonication. Structural changes of CR during the process of interaction with GO should go through several stages. Initially, CR structures with remaining $-N=N-$ group should be prevailing (Fig. 16, structure VI), later on, structural rearrangements, which increase the absorption above 640 nm are more probable (Fig. 16, structures III–V) (Fig. 15c).

Data obtained by UV-Vis and potentiometric titration experiments show that interaction between GO and CR molecules is accelerated by the sonication. In the sonicated GO-CR mixtures CR molecules adsorbed on the surface of GO sheets (with

transformation in their structure) are able to stabilize the aqueous suspensions. Ionization of the GO particles with adsorbed CR molecules leads to the significant changes in their conformation.

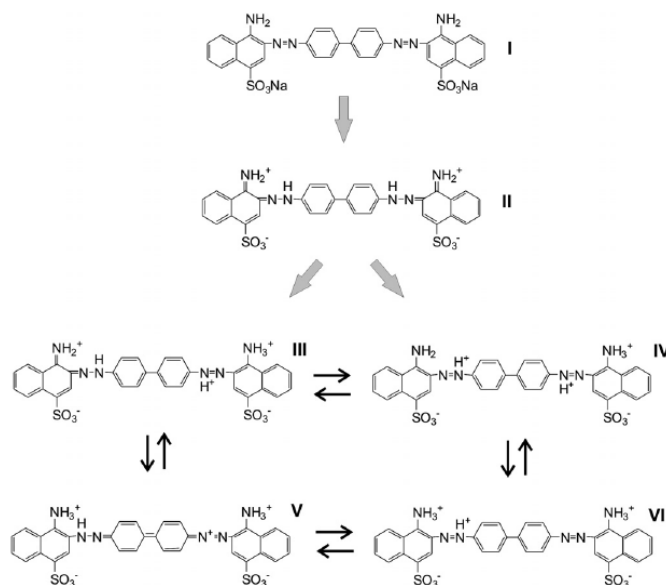


Fig. 16 Structural changes in CR molecules

3.2.2.2. Characterization of graphite oxide and Congo red nanocomposite films and coatings

The GO and GO/CR nanocomposite films and coatings were analyzed with SEM, XRD, FT-IR spectroscopy, Raman spectroscopy and CAM. The structure and properties of GO/CR nanocomposite coatings depend on the GO to CR ratio and preparation conditions. The samples with higher CR content were more flexible and prone to curl. GO and GO/CR coatings and films prepared from non-sonicated aqueous mixtures were more brittle in comparison with those prepared from sonicated mixtures.

SEM images show correlative changes in morphology of the nanocomposite films depending on the GO to CR ratio (Fig. 17). The films of GO and GO/CR show paper-like structure composed of ordered GO nanosheets. Fragments of the fracture for samples GO/CR exhibits a denser stacking of GO nanosheets in comparison with the coating without CR. The increasing in the CR concentration results in the arrangement of even denser stacking of GO nanosheets. Lateral view of GO5/CR* (Fig. 17l) reveals a brittle fracture line of the nanocomposite produced without sonication in comparison with the GO5/CR film of the same composition produced including the sonication

protocol. Regular changes in the morphology of GO/CR nanocomposite films indicate about a direct interaction between the GO particles and CR molecules and the role of the sonication process to formation of GO/CR nanocomposite structures. Sonication should be able to assist the penetration of CR molecules among the GO stacks.

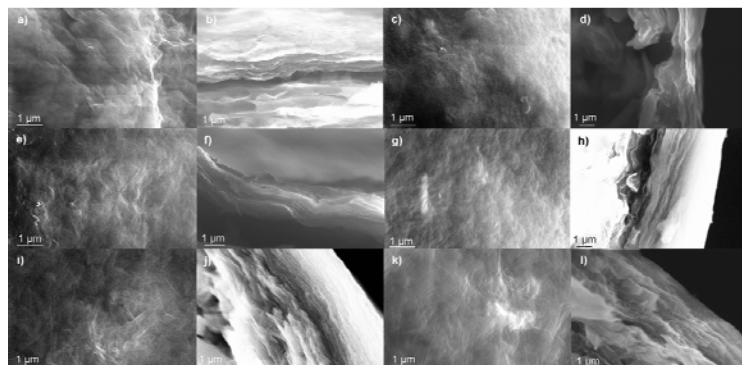


Fig. 17 SEM images of GO/CR nanocomposite films obtained at different fraction of CR: a), b) GO1; c), d) GO2/CR; e), f) GO3/CR; g), h) GO4/CR; i), j) GO5/CR; k), l) GO5/CR*

In Fig. 18a the FT-IR spectra of GO, CR and CR/GO nanocomposite coatings are presented. The most characteristic features are broad intense band at 3400 cm^{-1} (O–H stretching vibrations) and the bands at 1730 cm^{-1} (C=O stretching vibrations from carboxyl group), 1615 cm^{-1} (skeletal vibrations from non-oxidized graphitic domains), 1226 cm^{-1} (C–OH stretching vibrations), and 1055 cm^{-1} (C–O–C stretching vibrations). The absorption bands near 3450 and 1611 cm^{-1} in the FT-IR spectrum of solid state CR were assigned to stretching vibration of N–H and –N=N– bonds, respectively. The bands at 1227 cm^{-1} might be associated with the stretching vibrations of =C–N= group adjacent to aromatic ring. The absorption bands near 1364 and 1047 cm^{-1} were assigned to asymmetrical and symmetrical stretching vibration of S=O bonds in $-\text{SO}_3^-$ group. Appropriate changes in the FT-IR spectra of CR/GO mixtures with different quantities of CR are apparent. The bands representing sulfonate group keep unchanged position. From this it can be concluded that the sulfonate functional group do not interact with GO nanoparticles during the adsorption process. Transformations of different type are observed in the region of bands representing vibrations of nitrogen atom. Such changes suggest involvement of N–H groups into interaction with GO. The band representing characteristic C–O–C vibrations disappears at higher ratios of CR. The band of GO at 1226 cm^{-1} is likely covered by the band of CR at 1227 cm^{-1} . The band at 1730 cm^{-1}

gradually decreases with the increase of the ratio of CR except for the sample GO2/CR, indicating the interaction of carboxyl groups of GO with ammonium groups of dye molecules.

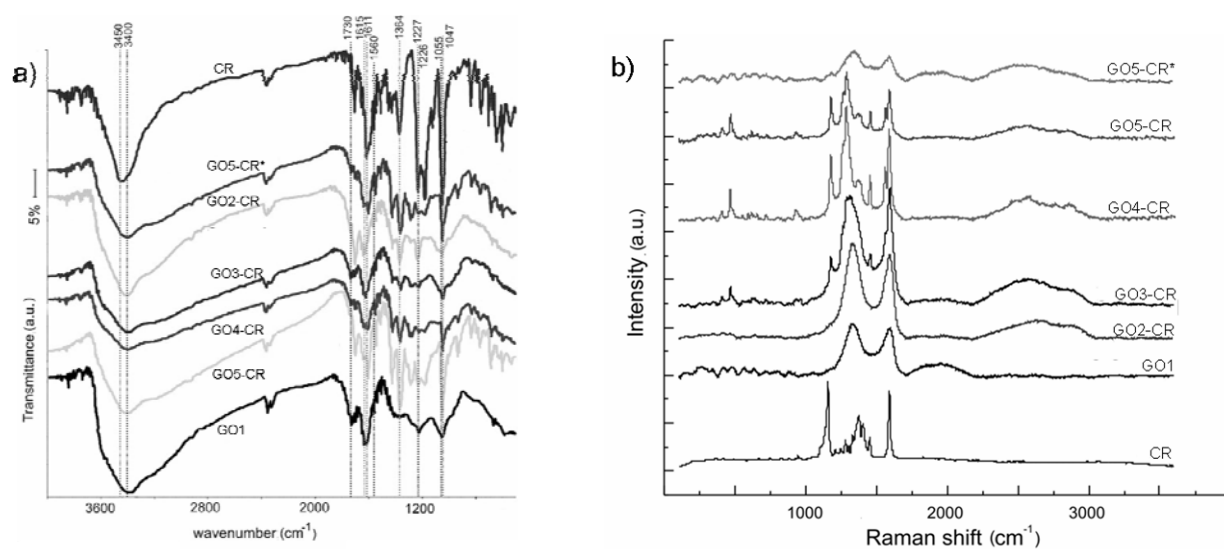


Fig. 18 a) FT-IR spectra of GO, CR and GO/CR nanocomposite coatings; b) Raman spectra of GO, CR and GO/CR nanocomposite coatings

Raman spectra of GO, CR and GO/CR nanocomposite coatings are presented in Fig. 18b. Two main peaks assigned to G (1580 cm^{-1}) and D bands ($1310\text{--}1430\text{ cm}^{-1}$) are prominent in GO and GO/CR nanocomposite samples. With the increase of CR proportion in the nanocomposite, Raman bands called 2D and D+G, located at $2700\text{--}3000\text{ cm}^{-1}$, appear. Our result indicates that due to the increased intensity of 2D band in Raman spectra, the size of sp^2 domains is increased after addition of small amounts of CR (up to 18,8 %). The excess of CR tends to reduce the intensity of 2D and D+G Raman bands. Raman analysis revealed a quinoid-like structure of CR dye in the GO/CR nanocomposites.

The XRD results of GO/CR nanocomposite coatings are shown in Fig. 19a. Inlet in Fig. 19a demonstrates the shape of the XRD peaks at $2\theta \approx 11^\circ$ in more details. XRD analysis shows that GO/CR nanocomposite samples obtained using different GO to CR ratios have different structural characteristics. Interplanar distances gradually increase (from 8,009 to 8,202 Å) with increasing CR portion in the nanocomposite. It may be assumed that the CR molecules are able to replace water molecules from the interplanar space of GO sheets. The procedure of sonication promotes direct interaction between GO functional groups and CR molecules. The size of crystallites runs through a maximum

(114,9 Å) with increasing the portion of CR in the nanocomposites. Small amounts of CR (up to 4,44 %) act positively on the formation of the larger crystallites, while the more significant portions of CR act in the opposite direction. We can consider that CR molecules interacting with the functional groups attached to the edges of GO sheets are able to combine them into larger units.

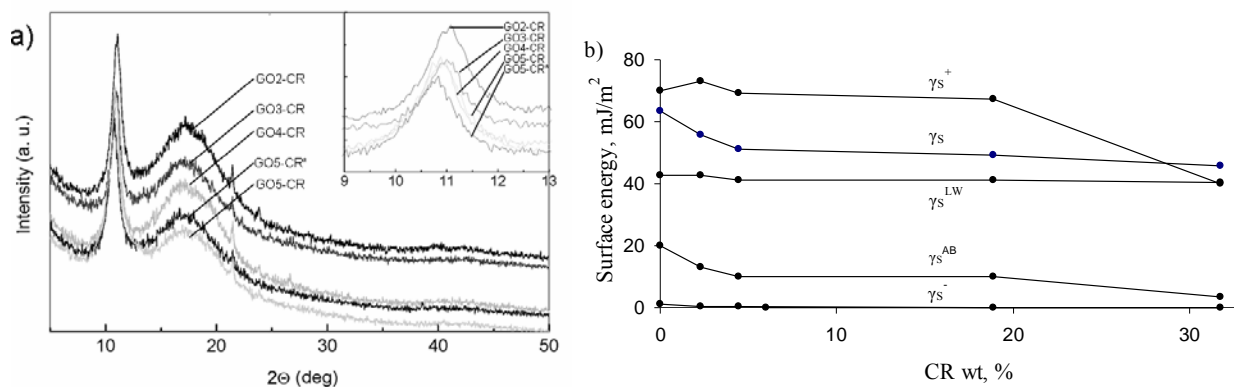


Fig. 19 a) XRD patterns of GO, CR and GO/CR nanocomposite coatings; b) surface energy dependence on the CR amount in GO/CR nanocomposite films

Data on the surface energy components and subcomponents and their dependence on the amount of CR in GO/CR nanocomposite films are presented in Fig. 19b. Total surface energy determined for the film GO1 equals 63 mJ/m². Addition of CR to GO/CR nanocomposite coatings leads to decrease of the total surface energy. Most probably, observed shift is related to the structural changes during the formation of the more compact GO/CR nanocomposite. Also, the data presented in Fig. 19b show that the surface of GO film is non-polar ($\gamma_S^{LW} > \gamma_S^{AB}$) with a big amount of acidic sites ($\gamma_S^+ > \gamma_S^-$, $\gamma_S^+ \approx 69$ mJ/m²). The addition of CR in GO/CR nanocomposites leads to decrease values of the surface free energy components and subcomponents. Supposedly CR molecules, being incorporated between basal planes, are able to reduce γ_S^+ values by increasing electron density in the single layer of GO.

In summary, GO/CR coatings prepared on the PC substrate were flexible, while the GO/CR films were brittle. It was estimated that CR addition formed a compact structure of nanocomposites due interaction functional groups of GO with amino groups of the CR molecule while sulfo groups tended not to react. According to our experiment data, small amounts of CR (up to 4,44 %) act positively on the formation of larger crystallites, while

more significant portions of CR act in the opposite direction. GO films exhibit non-polar character with a big amount of acidic sites on its surface.

Conclusions

1. MWCNTs were successfully synthesized by catalytic CVD method. SEM analysis of as-grown MWCNT samples showed morphology dependent on the synthesis conditions, such as catalyst precursor and synthesis temperature. The >100 nm in diameter MWCNTs with a big amount of impurities were obtained in the synthesis using carbonyl iron (particle size 4,5–5,2 μm) as a catalyst precursor. The <100 nm in diameter MWCNTs were synthesized on the nanodispersed particles of Fe and Ni catalysts, which were produced by thermal decomposition of ferrocene and NiC_2O_4 precursors, respectively. The optimal conditions to produce MWCNTs <100 nm diameter with the smallest amount of impurities are the catalytic reaction of ferrocene, *o*-xylene and CH_4 mixture at 650–850 $^\circ\text{C}$.
2. The samples of CNT were purified by treatment with CCl_4 and mixture of concentrated $\text{H}_2\text{SO}_4/\text{HNO}_3$ acids. The purification of CNTs by using CCl_4 is suitable and effective method to remove catalyst impurities (were determined by EDS, GA and magnetic balance measurements). Moreover, the analysis of the samples by EDS, FT-IR spectroscopy and Eschka titration methods showed that purification with CCl_4 method leads to surface modification with Cl^- functional groups, which increases the chemical activity (were determined by Boehm's titration method) and the solubility in aqueous solvents without the damage of surface structure of CNTs (showed the results of XRD and Raman spectroscopy). The purification with $\text{H}_2\text{SO}_4/\text{HNO}_3$, in contrast to purification procedure with CCl_4 , cuts CNTs, damages the surface structure (were determined by XRD) and introduces oxygen functional groups on the walls of nanotubes (were defined by FT-IR spectroscopy and Boehm's titration methods).
3. GO was synthesized by Hummer's method. XRD and Raman spectroscopy analysis showed that the degree of crystallinity of GO is very low. FT-IR spectroscopy and UV-Vis spectroscopy revealed the presence of hydroxyl, carboxyl and epoxy groups and non-oxidized regions in GO structure. XRD analysis of the sample showed that

the interlayer spacing of GO is expanded by H₂O molecules, intercalated between graphene sheets. Potentiometric titration experiments showed that GO in aqueous solution behaves as a weak polyfunctional acid ($pK_a = 6,22$). It was also indicated a very big influence of electrostatic repulsion between functional groups.

4. MWCNT coatings were produced by catalytic CVD method on the polished quartz and MgO substrates. Furthermore, the coatings were fabricated on both MgO/PVA and epoxy resin (EP) substrates from MWCNT aqueous suspensions. SEM analysis showed that the morphology of the CNT coatings strongly depends on the synthesis parameters (catalyst precursor and temperature). Higher synthesis temperatures (up to 900 °C) induce the growth of larger diameter MWCNTs. The coatings of <100 nm in diameter MWCNTs were produced using catalyst precursors such as ferrocene, pentacarbonyliron, NiC₂O₄ and Fe, Co and Ni phthalates. CAM analysis revealed that surface properties of the coatings depend on the amount and nature of functional groups attached to CNTs' walls. The results of CAM showed that the coatings of as-grown MWCNTs are hydrophobic, while the coatings of functionalized MWCNTs are more hydrophilic. The coatings formed from CNTs treated with CCl₄ exhibit a less hydrophilic character in comparing with the coatings formed from functionalized CNTs. The surface of CNT coatings purified with CCl₄ is non-polar with a big amount of acidic sites. The surface acidity increases after modification with oxygen containing functional groups.
5. The nanocomposite films and coatings of various GO to CR ratio were prepared from aqueous suspensions by filtering in water through a PC membrane filter. Data obtained by UV-Vis and potentiometric titration experiments showed that interaction between GO and CR molecules is accelerated by the sonication. The interaction between GO particles and CR molecules is suggested to stabilize the aqueous suspensions of GO sheets. Potentiometric titration data revealed that ionization of GO particles with adsorbed CR molecules leads to the significant changes in their conformation. SEM analysis of GO/CR films indicated that CR addition formed a compact structure of nanocomposites. XRD, Raman and FTIR measurements showed that amino groups in the CR molecule were able to interact with functional groups of GO. Raman analysis revealed a quinoid-like structure of CR dye in the GO/CR

nanocomposites. It was found that the small amounts of CR (up to 4,44 %) act positively on the formation of GO/CR films and coatings. The results of CAM showed that the GO films exhibit non-polar character with a big amount of acidic sites on its surface.

The list of original publications by the author

Articles in journals

1. J. Barkauskas, **I. Žaržojūtė**, A. Kareiva. Production and contact angle measurement of nano-structured carbon coatings. *Chemija*, **18** (2) (2007) 12–16.
2. J. Barkauskas, **I. Stankevičienė**. Synthesis of vapour-grown micrometer-scale carbon fibers. *Mendeleev Communications*, **19** (3) (2009) 123–125.
3. J. Barkauskas, **I. Stankevičienė**, A. Selskis. A novel purification method of carbon nanotubes by high-temperature treatment with tetrachloromethane. *Separation and Purification Technology*, **71** (3) (2010) 331–336.
4. J. Barkauskas, **I. Stankevičienė**, J. Dakševič, A. Padarauskas. Interaction between graphite oxide and Congo red in aqueous media. *Carbon*, **49** (15) (2011) 5373-5381.
5. J. Barkauskas, J. Dakševič, R. Juškėnas, R. Mažeikienė, G. Niaura, G. Račiukaitis, A. Selskis, **I. Stankevičienė**, R. Trusovas. Nanocomposite films and coatings produced by interaction between graphite oxide and Congo red. *Journal of Materials Science*, **47** (15) (2012) 5852-5860.

Published contributions to academic conferences

1. V. Goštautaitė, T. Trociukas, **I. Žaržojūtė**. The production of nano-structured carbon coatings. Vilnius university conference of young chemists „Inorganic compounds: synthesis, properties and application“. Varėnos dis., Burokaraistėlės vil., Lithuania, December 16-17 (2006) 35.
2. **I. Žaržojūtė**, J. Barkauskas. The surface of carbonaceous films evaluation using contact angle measurements. Conference „Chemistry and Technology of Inorganic Compounds“. Kaunas, Lithuania, April 25 (2007) 41-42.
3. J. Barkauskas, **I. Žaržojūtė**, R. Chalkovskaja. Thin layers of carbon nanotubes produced from methane precursor. The 9-th International Conference-School „Advanced materials and technologies“. Palanga, Lithuania, August 27-31 (2007) 57.

4. **I. Stankevičienė**, I. Grigoravičiūtė, J. Barkauskas. Synthesis, purification and functionalization of multi-walled carbon nanotubes. Conference „Chemistry and Technology of Inorganic Compounds“. Kaunas, Lithuania, April 22 (2009) 21-22.
5. **I. Stankevičienė**, J. Barkauskas. Synthesis and purification of carbon nanotubes. 9-th National Lithuanian Conference „Chemistry 2009“. Vilnius, Lithuania, October 16 (2009) 46.
6. J. Barkauskas, **I. Stankevičienė**, J. Dakševič, R. Trusovas, G. Račiukaitis, R. Mažeikienė. Interaction between graphite oxide nanoparticles and functionalized molecules: a way to produce and/or stabilize graphene coatings. International Conference „Carbon 2011“. Shanghai, China, 24-29 July (2011).
7. R. Trusovas, G. Račiukaitis, R. Mažeikienė, J. Barkauskas, **I. Stankevičienė**, J. Dakševič. Thermal Conductivity of Laser-treated Graphene/Graphite oxide Coatings. International Conference „Carbon 2011“. Shanghai, China, 24-29 July (2011).

CURRICULUM VITAE

Inga Stankevičienė

2000–2004 Bachelor Studies at Pedagogical University, Faculty of Natural Sciences – Bachelor Degree in Chemistry and Teacher's Professional Qualification.

2004–2006 Master Studies at Vilnius University – Master Degree in Chemistry.

2006–2012 Postgraduate studies at the Department of General and Inorganic Chemistry, Faculty of Chemistry of Vilnius University.

ANGLINIŲ NANOSTRUKTŪRŲ SINTEZĖ IR DANGŲ GAMYBA

Santrauka

Anglinių nanodarinių savybės ir pritaikymo galimybės priklauso nuo pasirinkto sintezės metodo ir sąlygų. Mūsų laboratorijoje DANV ir jų dangos buvo susintetintos paprastu, lengvai kontroliuojamu katalitiniu CVD metodu, o GO buvo pagamintas saugiu ir plačiausiai naudojamu Hummers'o metodu. Nepaisant katalitinio CVD metodo privalumų, kartu su sintezės produktu aptinkamos katalizatoriaus priemaišos, kurios apriboja ANV pritaikymą įvairiose srityse. Norint greitai ir efektyviai išvalyti ANV nuo Fe katalizatoriaus priemaišų, pirmą kartą buvo pritaikytas valymas CCl_4 garais. Papildomai ANV buvo išvalyti $\text{H}_2\text{SO}_4/\text{HNO}_3$ mišiniu.

Ištyrus susintetintą produktą SEM metodu buvo nustatyta, kad mažo skersmens DANV susidarymą labiausiai įtakoja katalizatoriaus pirmtakas ir sintezės temperatūra. SEM, XRD, Raman'o sklaidos spektroskopijos, GA, EDS metodais ir sveriant magnetinėmis svarstyklėmis buvo nustatyta, kad optimalios sąlygos susidaryti iki 100 nm skersmens, aukšto kristališkumo, mažai struktūrinių defektų ir priemaišų turintiems DANV yra feroceno, *o*-ksileno ir CH₄ reakcijos 650–850 °C temperatūroje. XRD, EDS, GA tyrimų metodais ir sveriant magnetinėmis svarstyklėmis buvo nustatyta produkte esančių katalizatoriaus priemaišų kiekis ir sudėtis. Ištyrus išvalytą produktą Raman'o sklaidos spektroskopijos, FT-IR spektroskopijos, Boehm'o titravimo ir Eschkos titravimo metodais buvo pagrįstas valymo CCl₄ garais metodo efektyvumas. Susintetinti ir įvairiais metodais išvalyti DANV buvo panaudoti dangų ant MgO/PVA ir EP pagrindo gamyboje. Taip pat, DANV dangos ant šlifluoto kvarco ir MgO padėklų buvo susintetintos katalitiniu CVD metodu.

Ištyrus GO XRD, Raman'o sklaidos spektroskopijos, FT-IR spektroskopijos ir UV-Vis spektroskopijos metodais buvo nustatyta, kad jo struktūroje yra didelis defektų kiekis, o paviršiuje yra oksiduotų ir neoksiduotų sričių. Siekiant pagaminti ilgą laiko tarpą stabilias vandenines suspensijas, GO paviršius buvo modifikuojamas CR dažo molekulėmis. GO ir GO/CR nanokompozitinės plėvelės ir dangos ant PC membraninio filtro buvo pagamintos laboratorijoje sukurtu filtravimo į tirpalą metodu.

Ištyrus DANV dangas SEM ir CAM metodais buvo nustatyta, kad dangų morfologija priklauso nuo sintezės sąlygų, o paviršiaus savybės nulemia prisijungusių funkcinių grupių pobūdis ir kiekis. CAM tyrimas atskleidė, kad dangų, kurias sudaro susintetinti DANV, paviršius yra nepolinis su skirtingu rūgštinių ir bazinių sričių santykiu. Buvo pastebėta, kad rūgštinių sričių padaugėja dangose, kurias sudaro išvalyti DANV. Ištyrus GO ir GO/CR nanokompozitines dangas ir plėveles SEM metodu buvo nustatyta, kad maži CR kiekiai skatina kompaktiškesnių nanokompozitų susidarymą ir stiprina dangų bei plėvelių patvarumą. Ištyrus GO ir CR molekulių sąveiką XRD, pH-potenciometrinio titravimo, FT-IR spektroskopijos, UV-Vis spektroskopijos ir Ramano spektroskopijos metodais buvo nustatyta, kad didesni kristalantai susidaro dėl GO funkcinių grupių sąveikos su CR molekulių amino- funkcinėmis grupėmis. CAM atskleidė, kad GO/CR nanokompozitinių plėvelių paviršius yra liofilinis, nepolinis su dideliu rūgštinių sričių kiekiu.